Available online at www.sciencedirect.com
ScienceDirect
Journal of Power Sources 173 (2007) 53–59
JOURNAL OF POWER SOURCES
www.elsevier.com/locate/jpowsour

Analysis of palladium-based anode electrode using electrochemical impedance spectra in direct formic acid fuel cells

Won Suk Jung [a], Jonghee Han [a], S. Ha [b,*]

[a] *Fuel Cell Research Center, Korea Institute of Science and Technology, 39-1 Hawolgok-dong, Seongbuk-gu, Seoul 136-791, Republic of Korea*
[b] *Department of Chemical Engineering, Washington State University, P.O. Box 642710, Pullman, WA 99164-2710, USA*

Received 6 April 2007; received in revised form 7 August 2007; accepted 8 August 2007
Available online 17 August 2007

Abstract

In this study, we used the electrochemical impedance spectra to evaluate the anode performance of direct formic acid fuel cell (DFAFC), and how its anode charge transfer resistance ($R_{anode,ct}$) and electrolyte resistance (R_{ele}) are affected by various cell operating parameters. The parameters investigated in this study include the anode overpotentials, cell operation times, formic acid feed concentrations and cell temperatures. The anode impedance spectra demonstrated that the $R_{anode,ct}$ and R_{ele} are low for the DFAFC using 5 M formic acid feed concentration, which leads to its high power density output of 250 mW cm^{-2} at 0.35 V and 30 °C. The high performance of the DFAFC demonstrates that it has a great potential for portable power applications. The $R_{anode,ct}$ increases gradually as either the cell operation time increases or the formic acid feed concentration is raised from 10 to 15 M, which leads to a deactivation of the anode electrode, resulting in reduction of overall cell performance. However, these deactivation processes are reversible and the cell performance can be easily reactivated.

Keywords: Direct formic acid fuel cells; Portable power; Impedance spectroscopy; Palladium; Charge transfer resistance; Electrolyte resistance

1. Introduction

Recently, considerable interest has developed in the use of miniature fuel cells as replacements for batteries in portable electronics. Miniature fuel cells offer the advantages of possessing much higher stored energy density and are able to be immediately recharged by replacing the fuel cartridge [1]. Most investigators explore direct methanol fuel cells (DMFCs) for this purpose [2,3], but our previous papers have demonstrated that direct formic acid fuel cells (DFAFCs) are remarkable for portable power applications as well [4–8]. Formic acid is a liquid-like methanol, but it has a lower crossover through the Nafion® membrane and a higher kinetic activity than methanol. These unique characteristics of formic acid allow us to operate DFAFCs at higher voltages than DMFCs. Methanol does have a higher theoretical energy density than formic acid. However, because fuel cells run more efficiently at higher voltages, in practice DFAFCs have similar energy density as DMFCs. Furthermore, DFAFCs have a power density in the range of three to six times greater than DMFCs, and operate well at room temperatures [4–8]. In recent reports, Ha et al. demonstrated that the DFAFC produces a maximum power density of 180 mW cm^{-2} at ambient temperature under a passive operation mode [9]. Under similar conditions, DMFCs produce a much lower power density than 180 mW cm^{-2}. Thus, DFAFCs have advantages over DMFCs. As a result of this unusually high power density, it was demonstrated that DFAFCs could also be used to power a laptop [10].

Impedance spectroscopy is a relatively new and powerful method of characterizing many of the electrical properties of materials and their interfaces. Recently, this analytical method was used to evaluate the electrochemical behavior of anode and cathode electrodes, in addition to electrolyte materials of hydrogen fuel cells and direct methanol fuel cells (DMFCs) [11–15]. Based on these electrochemical impedance analyses, electrochemical behaviors of these fuel cells were recognized in detail to optimize their power density and stability. However, in our current research, there is no investigation with regard to electrochemical impedance analysis of DFAFCs. Currently, there are gaps in the understanding of its low anode kinetics with

* Corresponding author. Tel.: +1 509 335 3786; fax: +1 509 335 4806.
E-mail address: suha@wsu.edu (S. Ha).

0378-7753/$ – see front matter © 2007 Elsevier B.V. All rights reserved.
doi:10.1016/j.jpowsour.2007.08.023

high formic acid concentrations, and its low anode stability for a long-term operation [8,16]. In this study, we use impedance spectroscopy to investigate the detailed electrochemical behaviors of DFAFC's anode under various operating conditions. The results of this study will provide essential information in improving both the performance and stability of existing DFAFCs.

2. Experimental

The membrane electrode assemblies (MEA) were fabricated in-house using a 'direct paint' technique as it is described in elsewhere [4–6,8]. The active area is 4 cm^2. The 'catalyst inks' were prepared by dispersing the catalyst powders into appropriate amounts of Millipore water and 5% recast Nafion® solution (1100EW, Solution Technology, Inc.). At that time both the anode and cathode 'catalyst inks' were directly painted onto either sides of the Nafion® 115 membrane. A commercially available platinum black (HiSPEC™ 1000 from Johnson Matthey) was used for the cathode catalyst layer at a loading of 7 mg cm^{-2}. Pd black (High Surface Area from Sigma–Aldrich) was used for the anode catalyst layer at a loading of 8 mg cm^{-2}. The final catalyst layers contained 15% Nafion® by weight.

The cell polarization was performed using a test fuel cell. Cell potential was controlled by a fuel cell testing station (University model, Fuel Cell Technologies. Inc.). The MEA was placed between two graphite plates with serpentine flow fields. Different concentrations of formic acid between 5 and 15 M were fed to the anode at a constant flow rate of 1 ml min^{-1}, while the cathode was supplied with a dry air at a flow rate of 400 sccm. Every experiment was operated at 30 °C except when specified otherwise.

The anode polarization curves were acquired by replacing the dry air gas stream at the cathode with H_2. The anode potential was stepped from 0 to 1.25 V in 50 mV increments at 5 s intervals using a Hewlett-Packard, model 6033 A, power box. The Pt/H_2 combination on the cathode side of the test fuel cell acted as a dynamic hydrogen reference electrode (DHE), as well as a high surface area counter electrode. The H_2 flow was maintained at a rate of 100 sccm, under a backpressure of 10 psi, and humidified at 45 °C prior to entering the cell. Formic acid was supplied to the anode side of the test fuel cell, at a flow rate of 1 ml min^{-1}, with the anode catalyst acting as the working electrode for the electrochemical cell.

Fig. 1 illustrates the electrochemical setup used in this investigation to perform the impedance spectroscopy measurement. The frequency response analyzer (FRA, Solartron1260) was used in this work and controlled by personal computer. It was coupled to a potentiostat (Solartron 1286) to support the modulation of dc current. We typically took impedance spectra between 50 kHz and 5 mHz with 10 steps per decade. For all the impedance spectroscopy measurements, various concentrations of formic acid were fed to the anode at a flow rate of 1 ml min^{-1} while hydrogen gas was supplied to the cathode at a flow rate of 200 sccm. This allowed us to eliminate the effect of the cathode impedances, and to investigate only the anode impedances of the cell as the cell operation parameters are varied. To avoid inductance among lines, we used the shortest lines possible and made certain they were not intertwined.

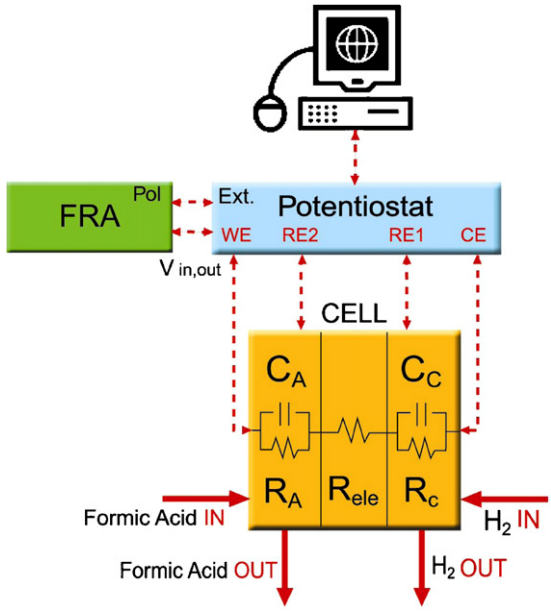

Fig. 1. Experimental setup for measuring anode electrochemical impedance spectroscopy of DFAFCs.

3. Results and discussion

3.1. Influence of the anode overpotential on the anode impedance spectra of the DFAFC

In Fig. 2, the anode impedance spectra of the DFAFC were measured using three different anode overpotentials: 0.1, 0.15 and 0.3 V versus DHE. For each anode impedance spectrum, 5 M formic acid was fed to the anode at ambient temperature. As shown in Fig. 2, the diameter of the semi-circle of each anode impedance spectrum can be measured by extrapolating their last

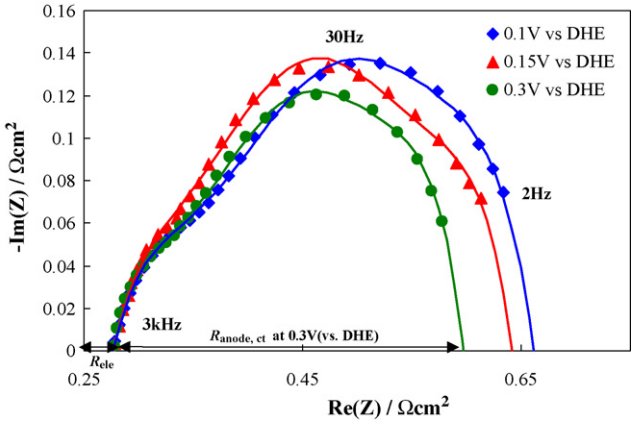

Fig. 2. Anode electrochemical impedance spectroscopy (Nyquist plots) of DFAFCs at various anode overpotentials of 0.1, 0.15 and 0.3 V (vs. DHE) were measured at ambient temperature. The 5 M formic acid was fed to the anode at a flow rate of 1 ml min^{-1}. To set the cathode as DHE, H_2 of 200 sccm was supplied to the cathode. For each spectrum, the frequency was varied from 2 Hz to 3 kHz.

points in the low frequency region to the x-axis. The diameter of the semi-circles in Fig. 2 are referred to as the anode charge transfer resistances, $R_{anode,ct}$, while the intersection points on the x-axis in their high frequency regions are referred to as the electrolyte resistances, R_{ele}. For the formic acid oxidation reaction, the surface of the Pd-based anode electrode is partially covered by adsorbed CO (not shown in figures). We speculate that the adsorbed CO (or other adsorbed intermediates) on the surface of the Pd catalyst creates an inductance effect. This inductance effect causes the impedance plots in Fig. 2 look as though they are composed of two semicircles [17]. To understand the origin of this two-semicircle effect in Fig. 2 in more detail, additional investigations are needed in the future. According to Fig. 2, the $R_{anode,ct}$ decreases as the anode overpotential increases from 0.1 to 0.3 V versus DHE. This is because the activation kinetics improve by increasing the anode overpotential. On the other hand, Fig. 2 also shows that R_{ele} remained unchanged at a constant value of 0.265 Ω cm^2. It is interesting to note in Fig. 2 that $R_{anode,ct}$ is very small, even at the low anode overpotential compared to DMFCs. For example, $R_{anode,ct}$ is only 0.662 Ω cm^2 at the anode overpotential of 0.1 V, which indicates fast oxidation kinetics for formic acid on the Pd catalysts in the DFAFCs. Under similar conditions, $R_{anode,ct}$ of DMFC was over 1.5 Ω cm^2 even at a higher anode potential of 0.2 V versus DHE using a Pt/Ru catalyst [18].

3.2. *Effect of anode deactivation on the anode impedance spectra of the DFAFC*

In Fig. 3, the initial cell polarization and the power density plots (blue plots) of the DFAFC are measured using 5 M formic acid and dry air at 30 °C. According to Fig. 3, the DFAFC produces a maximum power density of 250 mW cm^{-2} at 0.35 V. This performance is superior to any existing direct liquid organic fuel cells under similar conditions. Immediately after this initial cell polarization, the hydrogen gas was supplied (rather than dry air) to the cathode at 30 °C to make the cathode a DHE. Then, a constant anode potential of 0.15 V versus DHE was applied to the anode and its anodic current density was measured over 80 min as it is shown in Fig. 4(A). During this constant anode overpotential test, the anode impedance spectra were also measured simultaneously. Since it takes 20 min to measure one impedance spectrum, a total of four impedance spectra were measured over the 80 min as shown in Fig. 4(B). After the 80 min, the cathode gas was switched back to the dry air from the hydrogen. The cell polarization and the power density plots (red plots) of the used DFAFC were measured, as shown in Fig. 3. Both the $R_{anode,ct}$ and R_{ele} values are extracted from Fig. 4(B) and they are shown in Fig. 4(C) as a function of the cell operation time.

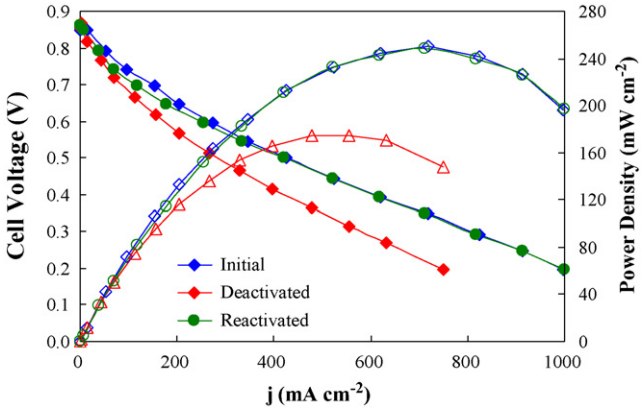

Fig. 3. Both *V–I* and power density plots were plotted for initial, deactivated and reactivated DFAFCs. The 5 M formic acid and dry air without backpressure were fed to the anode and cathode at flow rates of 1 ml min^{-1} and 400 sccm, respectively, at 30 °C. (For interpretation of the references to color in this figure citation, the reader is referred to the web version of the article.)

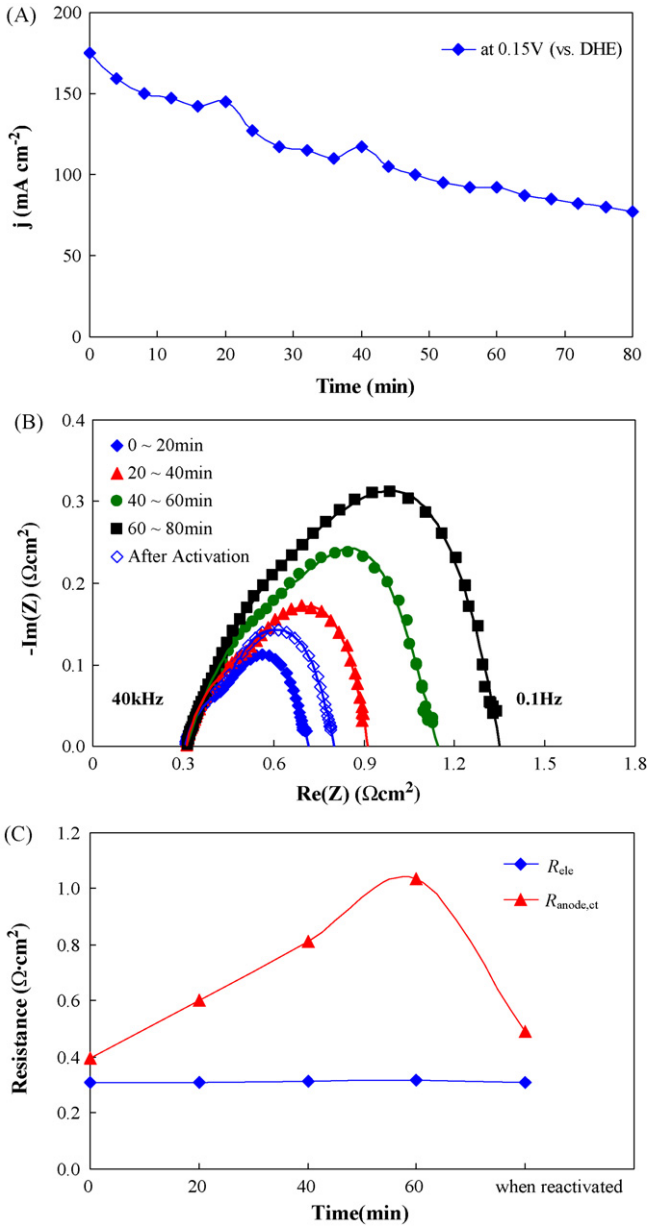

Fig. 4. Anode current density was plotted as a function of cell operation time (A) and anode electrochemical impedance spectroscopies were measured at fixed anode overpotential of 0.15 V vs. DHE for various cell operation times (B). The values of R_{ele} and $R_{anode,ct}$ at various cell operation times were extracted from above (C). The 5 M formic acid was fed to the anode at a flow rate of 1 ml min^{-1}. To set the cathode as DHE, H_2 of 200 sccm was supplied to the cathode.

According to Fig. 4(C), the $R_{anode,ct}$ increases by about 0.2 Ω cm^2 for every 20 min. As the $R_{anode,ct}$ increases over the 80 min, the anodic current density at 0.15 V versus DHE decreases from 175 to 80 mA cm^{-2} as shown in Fig. 4(A). Because of this anode deactivation, the overall cell performance also decreases as shown in Fig. 3. For example, according to Fig. 3, the cell current density and the power density at 0.35 V drop by 240 mA cm^{-2} and 75 mW cm^{-2} respectively as the cell's anode is deactivated over the 80 min test. Previous studies on the DFAFCs have pointed out that it is the Pd-based anode that provides the excellent performance, but its active surface is deactivated by an organic poisoning species over long operation time. These same studies also have indicated that this poisoning species is not carbon monoxide, but further investigation is needed to reveal its true identity [19]. We speculate that these same unidentified organic poisoning species cover up the active site of the Pd-based anode of our DFAFC as the cell operation time increases, which leads to its performance drop. Fig. 4(C) shows that the electrolyte resistance remained constant at a value of 0.32 Ω cm^2 while the anode deactivated over the 60 min period. This constant electrolyte resistance indicates that 5 M formic acid has enough water to prevent the Nafion® membrane from being dehydrated over these 60 min of the cell operation.

Ha et al. has demonstrated that the deactivated Pd-based anode of the DFAFC can be fully regenerated by applying a short high anodic potential (higher than 1.0 V versus DHE). Ha et al. speculated that the unidentified poisoning species are stripped off from the Pd surface by applying this high anodic potential [8]. In this study, we also applied the anodic potential of 1.0 V versus DHE for less than 3 s to the Pd-based anode electrode of the deactivated DFAFC. Both the current density and power density plots (green plots) of this reactivated DFAFC are also shown in Fig. 3. According to Fig. 3, the reactivated DFAFC is able to recover most of its initial power and current densities over the entire cell potential range. In addition, its $R_{anode,ct}$ value is dramatically decreased and very close to its initial value as shown in Fig. 4(B) and (C).

3.3. Effect of formic acid concentration on the anode impedance spectra of the DFAFC

Fig. 5 shows the effect of varying the formic acid feed concentration from 5 to 15 M on the cell polarization and cell power density curve profiles of the DFAFC at 30 °C. The largest current and power densities over the entire cell potential range that we studied are observed using a 5 M formic acid concentration. As the feed concentration of the formic acid is increased from 5 to 10 M, there are no changes in the kinetic regions (cell potential between 0.85 and 0.55). However, in the low cell potential region between 0.55 and 0.2 V, the DFAFC with 10 M formic acid produces much less current and power densities than with 5 M. As the formic acid concentration is further increased from 10 to 15 M, the current and the power densities of the DFAFC decrease over the entire cell potential range. Fig. 6 shows the anode polarization of the DFAFC using 5, 10 and 15 M formic acid at 30 °C. In general, Fig. 6 shows that the anode activity also decreases as the feed concentration of formic acid is increased

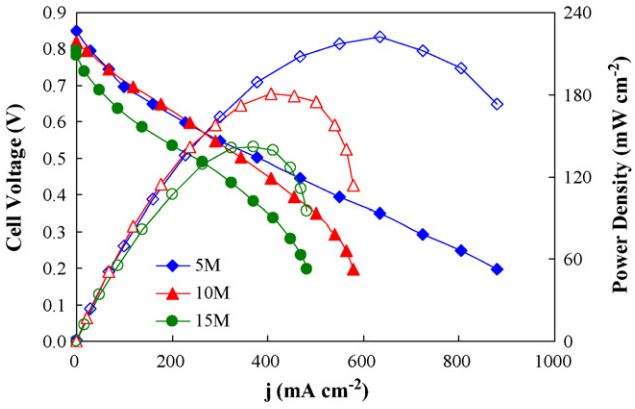

Fig. 5. Cell voltage and power density were plotted as a function of the current density using 5, 10 and 15 M formic acids. The formic acids and air were fed to the anode at a flow rate of 1 ml min^{-1} and 400 sccm, respectively, at 30 °C. The dry air was used without applying any backpressure.

from 5 to 15 M. To investigate the anode deactivation at high formic acid feed concentrations further, the anode impedance spectra of the DFAFC with 5, 10 and 15 M formic acid at a fixed anode potential of 0.15 V versus DHE were measured at various cell operation times (not shown in figures). In Fig. 7, the extracted values of the $R_{anode,ct}$ and R_{ele} for 5, 10 and 15 M formic acid feed concentrations from their impedance spectra are plotted as a function of the cell operation time at 30 °C. It is interesting to note that in Fig. 7(A) the R_{ele} of the DFAFC with 15 M formic acid is initially lower than the R_{ele} of the DFAFC with 5 and 10 M. However, the R_{ele} of the DFAFC with 15 M formic acid continuously increases as the operation time increases and it approaches the value of 0.54 Ω cm^2 after 15 min as shown in Fig. 7(A). Over the entire operation time, the R_{ele} of the DFAFC with 5 and 10 M are relatively unchanged. This indicates that the Nafion® membrane with 15 M formic acid takes a longer period to reach an equilibrium state when compared to the Nafion® membrane with 5 and 10 M formic acids. According to Fig. 7(A), after 15 min of the cell operation time, the R_{ele} is increased by 0.21 Ω cm^2 as the formic acid concentration is increased from 5 to 15 M. The R_{ele} increases due to the Nafion® membrane's dehydration effect at the high formic acid

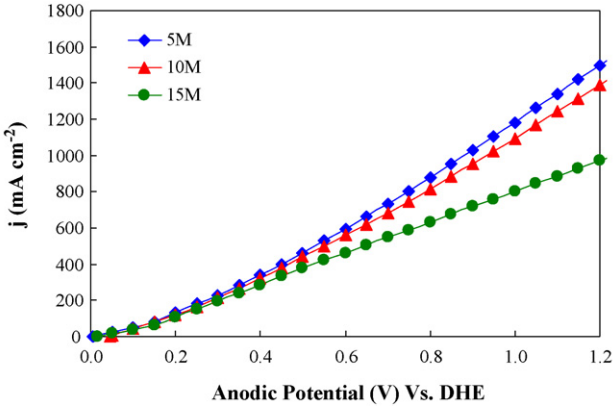

Fig. 6. Anode polarization plots were measured using 5, 10 and 15 M formic acids. The formic acid and dry H_2 were fed to the anode and cathode at flow rates of 1 ml min^{-1} and 200 sccm, respectively, at 30 °C.

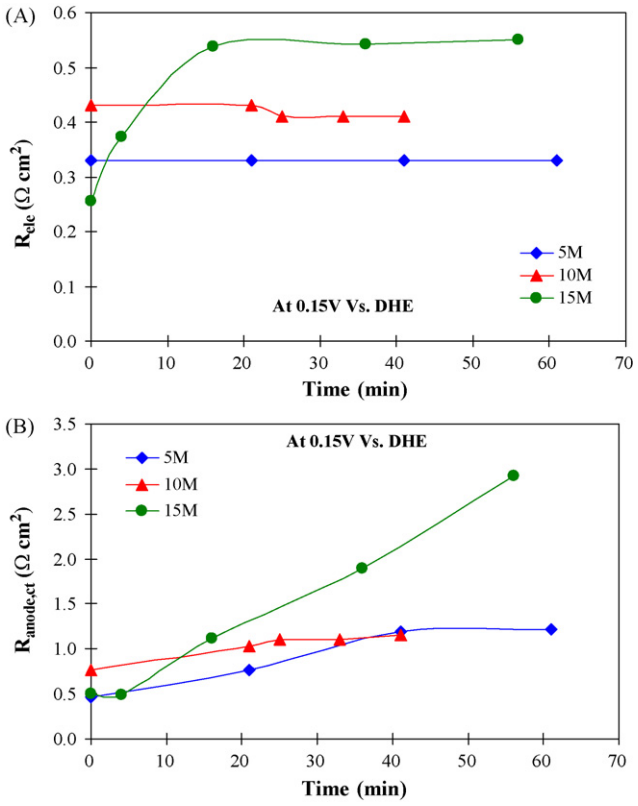

Fig. 7. The R_{ele} (A) and $R_{anode,ct}$ (B) of DFAFCs were plotted as a function of operation time for various concentrations of formic acid: 5, 10 and 15 M. The formic acids and dry H_2 were fed to the anode and cathode at flow rates of 1 ml min^{-1} and 200 sccm, respectively, at ambient temperature.

concentrations. The water content within the Nafion® membrane is decreased as the formic acid feed concentration at the anode is increased due to the hydroscopicity of concentrated formic acid. As the membrane is dehydrated, its resistance to proton flow also increases, which results in a higher value of R_{ele} with the higher concentrations of formic acid.

Fig. 7(B) shows that the $R_{anode,ct}$ of the DFAFC with 5 and 10 M formic acid feed concentrations increase slowly as the operation time increases, and they level off at the values of 1.20 Ω cm^2. On the other hand, the $R_{anode,ct}$ of the DFAFC with 15 M formic acid continuously increases without leveling off as the operation time increases as it is shown in Fig. 7(B). Based on Fig. 7(B), one can speculate that the formic acid oxidation kinetic on Pd catalysts is significantly changed when its concentration increases from 10 to 15 M. Zarakhani and Vinnik have reported that the dimer concentration of formic acid increases exponentially as its concentration is increased from 10 to 25 M [20]. The dimers would require a higher energy to be oxidized than the monomers, and the dimers and monomers would have different surface interactions with the Pd catalyst. Thus, the $R_{anode,ct}$ increases and shows the different trend as the formic acid concentration is increased from 10 to 15 M.

In order to investigate if the ascending and the descending order of varying the formic acid concentration have any effect on the membrane's dehydration level, we measured their impedance spectra by either increasing its concentration from 5 to 15 M or

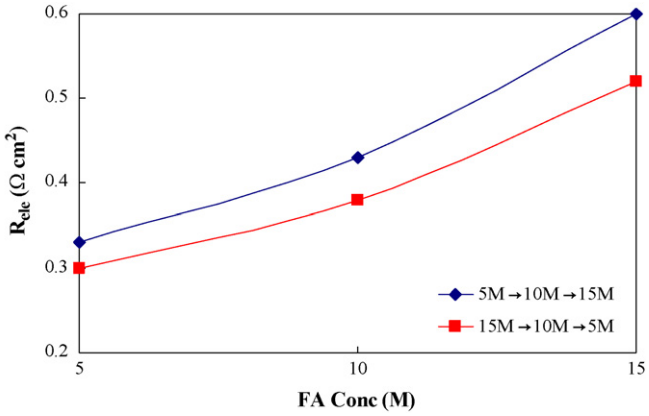

Fig. 8. The R_{ele} of DFAFCs were measured from their anode electrochemical impedance spectroscopy as a function of formic acid feed concentrations at ambient temperature. Both ascending and descending order of formic acid were used to measure the R_{ele} of DFAFCs in the figure (ascending order: 5 → 10 → 15 M and descending order: 15 → 10 → 5 M).

decreasing its concentration from 15 to 5 M. These results are summarized in Fig. 8 by plotting the R_{ele} as function of formic acid concentration for both the ascending and descending orders. According to Fig. 8, in both cases, the R_{ele} is higher with higher formic acid concentration. Based on Fig. 8, if the membrane is exposed to the high concentration of formic acid for less than 30 min, then its structures should not be permanently damaged and it can be easily re-hydrated by simply feeding excess water (or a lower concentration of formic acid).

The trends found in Figs. 5–7 are as follows: as the formic acid feed concentration is increased from 5 to 15 M, both the $R_{anode,ct}$ and R_{ele} increase. As the $R_{anode,ct}$ increases, the anode performance decreases and produces less current density. Due to the lower anode kinetic and higher electrolyte resistance at the high formic acid feed concentrations, the overall performance of the DFAFC decreases as its concentration is increased from 5 to 15 M as shown in Fig. 5.

The formic acid crossover flux is another possible reason that can explain the decreasing overall cell performance with the increased formic acid feed concentration. In our previous study, we have shown that the formic acid crossover flux through the Nafion® membrane increases slightly as the formic acid feed concentration is increased from 1 to 10 M [22]. However, in Fig. 5, the current density at the high cell potential range does not change significantly as the formic acid feed concentration is increased from 5 to 10 M. This indicates that the formic acid crossover flux does not affect the overall cell performance significantly as long as the formic acid feed concentration is maintained at 10 M or lower.

3.4. Effect of the cell temperature on the anode impedance spectra of the DFAFC

Fig. 9 plots both the cell polarization and power density curves of the DFAFC for varying cell temperatures. According to Fig. 9, both the cell current and power densities increase as the cell temperature increases from 30 to 45 °C. However, increa-

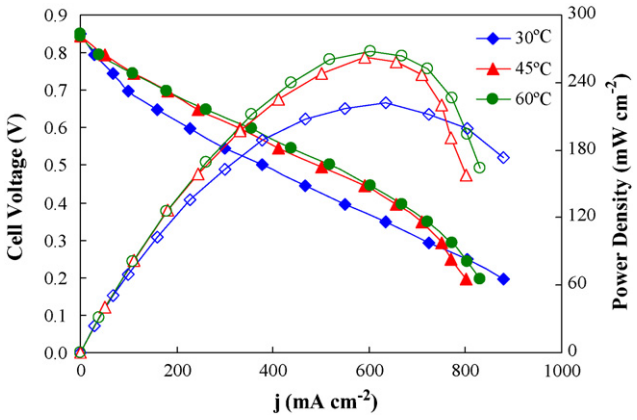

Fig. 9. Cell voltage and power density were plotted as a function of the current density at the cell temperatures of 30, 45 and 60 °C. The 5 M formic acid and dry air without applied backpressure were fed to the anode and cathode at flow rates of 1 ml min^{-1} and 400 sccm, respectively, at various cell temperatures.

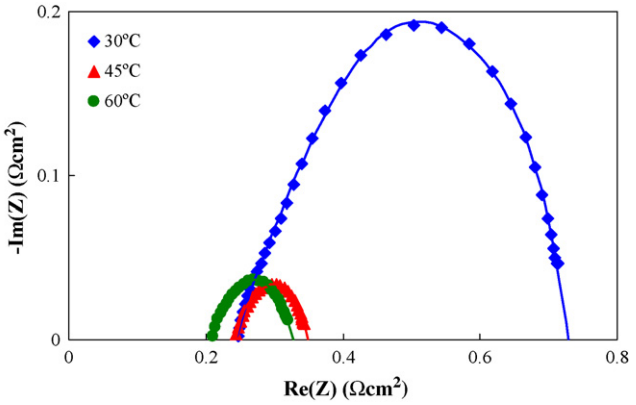

Fig. 11. Anode electrochemical impedance spectroscopies of DFAFCs were measured at fixed anode overpotential of 0.1 V vs. DHE for various cell operation temperatures. The 5 M formic acid and dry air without applied backpressure were fed to the anode and cathode at flow rates of 1 ml min^{-1} and 400 sccm, respectively, at the cell operation temperatures of 30, 45 and 60 °C.

sing the cell temperature beyond 45 °C does not increase the cell performance. Fig. 10 shows the anode polarization curves of the DFAFC for varying cell temperature. In Fig. 10, the anodic current density increases as the cell temperature increases from 30 to 45 °C. However, similar to the cell polarization and cell power density curve profiles, the anode performance does not enhance by further increasing the cell temperature to 60 °C. Fig. 11 shows the dependence of the anode impedance spectra of the DFAFC on the cell temperature. According to Fig. 11, the R_{ele} decreases as the temperature increases. This temperature effect on the R_{ele} can be explained in terms of the increased proton conductivity of Nafion® at the elevated temperatures. As long as Nafion® is not dehydrated, its proton conductivity increases as the temperature increases [21]. Thus, the lowest R_{ele} of DFAFC occurs at 60 °C in Fig. 11. According to Fig. 11, the $R_{anode,ct}$ decreases very significantly from 0.46 to 0.11 Ω cm^2 as the cell temperature increases from 30 to 45 °C. Further increasing the cell temperature to 60 °C does not decrease the $R_{anode,ct}$. Based on Figs. 9–11, it is apparent that the anode kinetic is enhanced by decreasing its $R_{anode,ct}$ as the cell temperature increases from 30 to 45 °C. This anode kinetic enhancement leads to increasing both the current and the power densities of the DFAFC as the cell temperature increases from 30 to 45 °C. However, it is very interesting to observe that there is no further improvement in the $R_{anode,ct}$ by increasing the cell temperature from 45 to 60 °C. Because of this, both the anode and overall performance of the DFAFC do not increase even though the cell temperature increases from 45 to 60 °C.

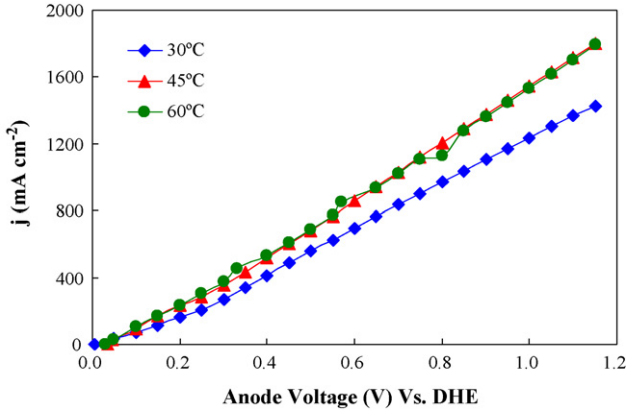

Fig. 10. Anode polarizations were measured at various cell temperatures ranging from 30 to 60 °C. The 5 M formic acid and dry air without applied backpressure were fed to the anode and cathode at flow rates of 1 ml min^{-1} and 400 sccm, respectively, at various cell temperatures.

4. Conclusion

In this study, the electrochemical impedance spectra have been successfully used as an in situ diagnostic tool for the DFAFC. The anode impedance spectra show that the anode charge transfer resistance ($R_{anode,ct}$) is very low even if its anode overpotential is small, which is indicative of a fast oxidation reaction of formic acid on the Pd catalysts. As the cell operation time increases, the $R_{anode,ct}$ increases gradually due to a strongly adsorbed poisoning species (non-CO species) on its Pd-based anode surface. This poisoned anode surface is easily reactivated by applying a high anodic potential of 1.0 V versus DHE. As the anode surface is reactivated, its $R_{anode,ct}$ decreases close to its initial value. The $R_{anode,ct}$ is also a function of the formic acid feed concentration and it increases dramatically as the formic acid concentration is increased from 10 to 15 M, which leads to a low performance of the DFAFC using 15 M formic acid. We speculate that the high concentration of dimer in 15 M formic acid is one of main reasons for increasing the $R_{anode,ct}$ of DFAFC as its feed concentration is elevated from 10 to 15 M. The R_{ele} is low if 5 M formic acid is used to operate the DFAFC. The R_{ele} increases gradually as the formic acid feed concentration is elevated due to the membrane dehydration. However, the membrane is easily re-hydrated by feeding excess water. In general, the cell temperature also has a positive effect on the $R_{anode,ct}$ and R_{ele}. The $R_{anode,ct}$ decreases as the cell temperature increases from 30 to 45 °C because of its increased kinetic at the higher temperature. Both the anode impedance spectra and anode polarization show that there is no further

anode kinetic gain as the cell temperature is increased from 40 to 60 °C.

Acknowledgements

This work was supported by the Korea Institute of Science and Technology and the Korea Research Foundation Grant (KRF-2006-612-D00021) funded by the Korean Government (MOEHRD).

References

[1] B.J. Feder, New York Times, New York, 2003.
[2] A. Blum, T. Duvdevani, M. Philosoph, N. Rudoy, E. Peled, J. Power Sources 117 (2003) 22–25.
[3] H. Chang, J.R. Kim, J.H. Cho, H.K. Kim, K.H. Choi, Solid State Ionics 148 (2002) 606–610.
[4] C. Rice, S. Ha, R.I. Masel, P. Waszczuk, A. Wieckowski, T. Barnard, J. Power Sources 111 (2002) 83–89.
[5] C. Rice, S. Ha, R.I. Masel, A. Wieckowski, J. Power Sources 115 (2) (2003) 229–235.
[6] S. Ha, B. Adams, R.I. Masel, J. Power Sources 128 (2) (2004) 119–124.
[7] Y. Zhu, S. Ha, R.I. Masel, J. Power Sources 130 (1–2) (2004) 8–14.
[8] S. Ha, R. Larsen, Y. Zhu, R.I. Masel, Fuel Cells 4 (4) (2004) 337–343.
[9] S. Ha, Z. Dunbar, R.I. Masel, J. Power Sources 158 (1) (2003) 129–136.
[10] C. Miesse, W. Jung, K. Jeong, J. Lee, J. Lee, J. Han, S. Yoon, S. Nam, T. Lim, S. Hong, J. Power Sources 162 (1) (2006) 532–540.
[11] J. Zhang, Y. Tang, C. Song, J. Power Sources 163 (1) (2006) 532–537.
[12] J. Qiao, M. Saito, K. Hayamizu, J. Electrochem. Soc. 153 (6) (2006) A967–A974.
[13] W. Chen, G. Sun, J. Guo, X. Zhao, S. Yan, J. Tian, S. Tang, Z. Zhou, Q. Xin, Electrochim. Acta 51 (12) (2006) 2391–2399.
[14] K. Furukawa, K. Okajima, M. Sudoh, J. Power Sources 139 (1–2) (2005) 9–14.
[15] T. Abe, H. Shima, K. Watanabe, Y. Ito, J. Electrochem. Soc. 151 (1) (2004) A101–A105.
[16] S. Ha, R. Larsen, R.I. Masel, J. Power Sources 144 (1) (2005) 28–34.
[17] N.-Y. Hsu, S.-C. Yen, K.-T. Jeng, C.-C. Chien, J. Power Sources 161 (2006) 232–239.
[18] J.T. Mueller, P.M. Urban, J. Power Sources 75 (1998) 139–143.
[19] Y. Zhu, Z. Khan, R.I. Masel, J. Power Sources 139 (1–2) (2005) 15–20.
[20] N. Zarakhani, M. Vinnik, Russ. J. Phys. Chem. 37 (11) (1963) 2550–2553.
[21] M.G. Santarelli, M.F. Torchio, Energy Convers. Manage. 48 (2007) 40–51.
[22] Y.W. Rhee, S. Ha, R.I. Masel, J. Power Sources 117 (1–2) (2003) 35–38.